Time-Resolved Ligand Exchange Reactions: Kinetic Models for Competitive Inhibitors with Recombinant Human Renin

Maurice M. Morelock,*,† Christopher A. Pargellis,‡ Edward T. Graham,§ Daniel Lamarre,‖ and Grace Jung⊥

Sections of Biophysics and Cellular Inflammation, Department of Inflammatory Diseases, and Information Services, Boehringer Ingelheim Pharmaceuticals, Inc., 900 Ridgebury Road, P.O. Box 368, Ridgefield, Connecticut 06877-0368, and Departments of Biochemistry and Medicinal Chemistry, Bio-Méga/Boehringer Ingelheim Research, Inc., 2100 rue Cunard, Laval, PQ, Canada H7S 2G5

The on and off rate constants (k_{on} and k_{off}) were determined for a series of peptidomimetic, competitive inhibitors of human renin using a novel binding assay. The method entails analyzing a pair of ligand exchange reactions in which a dansylated inhibitor serves as the fluorescent probe. The first in the pair of reactions involves preincubating renin with the probe and initiating the reaction by addition of a sample inhibitor; the second reaction involves preincubating renin with the sample inhibitor and initiating the reaction by addition of probe. Both reactions yield progress curves which contain complementary information concerning the k_{on} and k_{off} of each ligand. The two curves are fitted simultaneously using models derived from the differential rate equations describing the ligand exchange process. The k_{on} and k_{off} rate constants for the probe were 6.85×10^6 M^{-1} s^{-1} and 2.96×10^{-4} s^{-1}, respectively, giving a calculated K_d of 43.2 pM. The K_d values for the inhibitor series varied over 2 orders of magnitude (27–2320 pM), while the individual k_{on} (10^6–10^7 M^{-1} s^{-1}) and k_{off} (10^{-4}–10^{-3} s^{-1}) constants varied only over 1 order of magnitude.

Determination of binding constants for high-affinity receptor–ligand systems has always presented an experimental challenge. A common dilemma is that high-affinity ligands appear to have similar potencies, a result of the experimental limits placed on the assay by the receptor concentration, ligand solubility, etc. These circumstances restrict the acquisition of data pertinent to the characterization of these systems using current methodologies. The application of ligand exchange reactions, however, is proving to be a valuable technique in providing critical information on these high-affinity systems.[1] The ligand exchange experiment is performed by first saturating the receptor with one ligand and then adding a competing ligand. The reaction is allowed to reach equilibrium and then analyzed by measuring either the association or the dissociation of a labeled ligand, typically a chromophore or radionuclide. These equilibrium data can then be used to determine the true affinity of the sample ligand.

As relationships between drug structure and biological activity have been delineated by X-ray crystallography and synthetic efforts, compounds have become more and more potent, and binding constants in the picomolar or even femtomolar range are no longer unusual.[2] Hence, one potential use of ligand exchange reactions is in the evaluation of drug candidates. A recent example involved equilibrium measurements of enzyme–inhibitor interactions in which the enzyme was the aspartyl protease renin and the probe was an inhibitor labeled with a dansyl fluorophor.[1] After excitation at 280 nm, binding could be detected by observing changes in emission signal intensity of either

the enzyme (340 nm, Trp quench) or the probe (520 nm, energy transfer to dansyl moiety), and dissociation constants (K_d) for a series of potent inhibitors were determined. Although drug candidates are commonly ranked for potency according to their K_d's, the dissociation *rate* (k_{off}) may be the more critical parameter for the selection of a drug candidate, as lower k_{off} values translate into longer half-lives for an inactive receptor–ligand complex. Since K_d is the ratio of k_{off} to k_{on} many different pairs of k_{off}/k_{on} values can give the same K_d. Consequently, drug candidate selection based on K_d values alone would overlook those inhibitors exhibiting the longer off rates. To date, however, time-resolved analyses of ligand exchange reactions have usually been limited to dissociation reactions for the determination of k_{off}, calculating k_{on} from K_d.

In contrast to equilibrium constants, however, rate constants are much more difficult to determine as they require time-based experimental techniques for data acquisition and the implementation of complex mathematical equations for data analysis. Since time-resolved data can be acquired for extremely fast association as well as relatively slow dissociation reactions by either stopped-flow or conventional spectroscopy, respectively, ligand exchange studies with potential drug candidates should reveal critical information concerning their respective k_{on} and k_{off} rates. This work focuses on obtaining these rate constants for a series of potential drug candidates via ligand exchange reactions with renin, specifically the peptidomimetic, amido diol transition state inhibitors reported by Lavallee and Anderson.[3] Due to its unique substrate specificity for angiotensinogen, renin inhibition is an attractive target that may offer therapeutic advantages over angiotensin-converting enzyme (ACE) inhibitors and other antihypertensive agents. Moreover, the potential for attenuating the renin blockade at the first and rate-determining step of the renin–angiotensin–aldosterone system

---

* To whom correspondence should be addressed.
† Section of Biophysics.
‡ Section of Cellular Inflammation.
§ Information Services.
‖ Department of Biochemistry.
⊥ Department of Medicinal Chemistry.

(RAAS) remains to be explored, in light of the putative role of angiotensin II in altering vascular structure during long-standing hypertension. Thus, an intensive effort has been concentrated on the development of orally effective and long-acting inhibitors of renin.[4] This paper presents the theory for time-resolved ligand exchange reactions, outlines specific experimental designs, and is accompanied by experimental data and the evaluation of statistical fitting procedures for the determination of renin inhibitor rate constants.

Theory

The following equation is a generalized scheme for receptor–ligand exchange reactions as they pertain to enzyme–inhibitor interactions.

$$ED \rightleftharpoons D + E + I \rightleftharpoons EI \qquad (1)$$
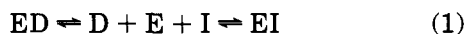
where E is the enzyme, D is the probe (e.g., dansyl-labeled) inhibitor, and I is the sample inhibitor. The individual equilibrium expressions for the above-generalized reaction scheme are given by the following equations:

$$E + D \underset{k_{1r}}{\overset{k_{1f}}{\rightleftharpoons}} ED \quad \text{where} \quad K_D = \frac{k_{1r}}{k_{1f}} = \frac{[E][D]}{[ED]} \qquad (2)$$

$$E + I \underset{k_{2r}}{\overset{k_{2f}}{\rightleftharpoons}} EI \quad \text{where} \quad K_I = \frac{k_{2r}}{k_{2f}} = \frac{[E][I]}{[EI]} \qquad (3)$$

where f and r refer to the forward (association) and reverse (dissociation) reactions, respectively. The dissociation constants K_D and K_I can be determined from an analysis of the enzyme species $[E]_\infty$, $[ED]_\infty$, and $[EI]_\infty$ in eq 1 at a time sufficient to achieve equilibrium conditions. It should be noted that the individual rate constants k_f and k_r can *not* be determined from equilibrium data.

In order to determine the rate constants, experiments need to be set up in such a way as to maximize the information concerning the specific steps of interest in the reaction scheme. For example, consider the experiment in which one of the inhibitors is preincubated with enzyme before addition of the other (and vice versa). The following two equations together constitute a *paired* receptor–ligand exchange reaction:

$$ED + I \rightleftharpoons EI + D \qquad (4)$$

$$EI + D \rightleftharpoons ED + I \qquad (5)$$
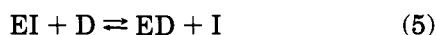
Note that the data obtained from the ligand exchange reaction involving dissociation of the probe (eq 4) principally contain information concerning the off rate of D and the on rate of I; conversely, data from the exchange reaction involving association of the probe (eq 5) are important in the determination of the on rate of D and the off rate of I. The complementary data from these two reactions can be combined in a *single* data set and then modeled simultaneously for the rate constants. (Note: For an example of paired progress curves as applied to inhibition of enzymatic activity, see Pargellis et al.[5]) The mathematical model for the paired receptor–ligand exchange reaction is given in Appendix 1.

Upon binding the enzyme, the probe ligand must (1) display a change in fluorescence signal large enough to

effectively detect changes in reactant concentrations and (2) maintain potency (as this sets the limit of the assay). In addition, the molecular structure and the biological activity of the probe should be similar to those of the inhibitor series of interest. Binding kinetics of a probe are typically monitored by observing changes in emission signal intensity at a fixed wavelength. A general equation for the fluorescence at time t describing the exchange ligand reaction can be written as follows:

$$F_t = (Q_{free}[\text{probe}]_{free}) + (Q_{bound}[\text{probe}]_{bound})$$

or

$$F_t = (Q_{free}([D]_{Total} - [ED]_t)) + (Q_{bound}[ED]_t) \qquad (6)$$

where Q_{free} and Q_{bound} are the relative quantum yields for the free and bound probe, respectively. Note that F_t can be written as a function of only one reaction species, namely [ED] at time t, and that the integrated rate equation for this species is given in Appendix 1.

In order to model data from paired receptor–ligand exchange reactions, a computational method is required that can (1) apply the appropriate nonlinear solution (as defined by reactant concentrations and order of addition) to each subset of the data, i.e., eq 4 or 5, and (2) iterate over the combined data set using both solutions simultaneously. This can be done using the 'MODEL' procedure available from SAS. A paired ligand exchange data set was simulated using the model given in Appendix 1 with ±0.5% normally distributed noise. If the nonlinear regression was applied solving for all four rate constants, the parameter estimates could not be determined with acceptable statistics, i.e., without bias and/or P values <0.05. Furthermore, if one of the rate constants was known, the other three could be determined but only when the regression involved a large body of data containing a broad range of inhibitor and enzyme concentrations. If, however, two rate constants were known, the other two could be determined with acceptable statistics from a *single* paired ligand exchange experiment. Thus, obtaining k_{1f} and k_{1r} for the probe is of particular interest. The mathematical model for determining the rate constants for the probe is given in Appendix 2.

In this study, the concentrations of the reactants were held constant for each of the paired ligand exchange reactions; consequently, both reaction curves in a set should converge to the same fluorescence value at equilibrium, i.e., $F_{t=\infty}$. Since experimental error in pipetting can lead to inequivalent E, D, and I concentrations for the two reactions in a paired set, the probe association and dissociation curves could be offset by a constant (Δ) relative to one another. Since Q_{free} and Q_{bound} are to be fitted for every paired ligand exchange data set, it becomes an arbitrary decision to correct the probe association or the probe dissociation curve by Δ. For this study, F_t was arbitrarily redefined for the probe dissociation reactions (eq 4) to be $F_t + \Delta$. Consequently, eq 6 becomes

$$F_t = (Q_{free}([D]_{Total} - [ED]_t)) + (Q_{bound}[ED]_t) - \Delta \qquad (6a)$$

for probe dissociation reactions, while F_t for the probe association remains defined by eq 6. These two equations (eq 6 and 6a) were applied simultaneously to
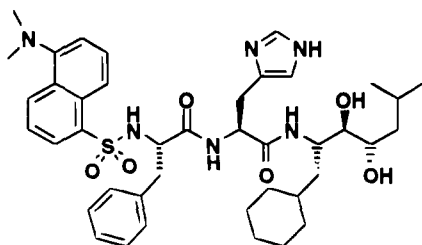
Figure 1. Structure of the fluorescent probe 1 used in ligand exchange studies with recombinant human renin.

paired reactions in the regression analysis, fitting for the rate constants of interest, the relative quantum yields, and Δ.

Results and Discussion

Epps et al.[1] have recently reported the use of a dansylated probe to characterize the binding phenomena for a series of potent inhibitors (picomolar range) of renin. These studies, however, were limited to equilibrium phenomena, i.e., K_d measurements. In the study reported herein, the emphasis was placed on the determination of the rates at which the receptor (renin) and ligands (inhibitors) proceed toward equilibrium, i.e., k_{on} and k_{off}. To this end, we have synthesized a dansylated ligand (1; see Figure 1) whose structure closely resembles the series of competitive (amido diol transition state analogs) renin inhibitors reported by Lavallee and Anderson.[3] In preliminary characterizations, 1 was shown to be a potent inhibitor by IC_{50} measurements (low nanomolar range) and to fluoresce at about 520 nm when excited at 325 nm (data now shown). Thus, the dansyl-labeled, amido diol 1 displayed an absorption-emission profile suitable for probing active-site phenomena while retaining potency.

The overlay of renin emission spectra is shown in Figure 2. With the excitation at 284 nm, renin alone (thick line) exhibits an emission maximum at about 325 nm (Trp emission). As 1 is added, an increase in emission at 520 nm is observed with a concomitant decrease at 325 nm, consistent with Trp quenching and energy transfer from Trp to the dansyl group. (Note: A small, but minimal, emission was observed for the highest concentration of 1 in the absence of renin at 520 nm.) The inset shows the linear decrease/increase at 340/520 nm, respectively, as a function of 1 added. As can be seen, renin binds 1 quantitatively at low stoichiometry and saturates at approximately a 1:1 binding ratio. Thus, the renin−1 complex could be quantitated at either 340 or 520 nm with approximately equal responses. Since changes in fluorescence at 520 nm offered the advantages of lower background and signal in absence of complex, 284 and 520 nm were chosen for excitation and emission, respectively. In this system, fluorescence at 520 nm increases as 1 binds renin and decreases as 1 dissociates from renin.

The stopped-flow experiments involving the association of 1 with renin are shown in Figure 3. The fluorescence increases rapidly and approaches saturation after about 2 s for the concentrations of 1 investigated. The fact that the progress curves do not start precisely at zero for the higher concentrations of 1 is due to an increased concentration of free probe and the 1.2 ms dead-time of the stopped-flow reactor. Nevertheless, the reactions appear to be monophasic with the initial slopes and the fluorescence plateau values increasing with higher concentrations of 1, accordingly. Kati[6] reported a two-step mechanism for peptidomimetic, competitive inhibitors of human renin in which an initial collision results in a loosely bound EI complex
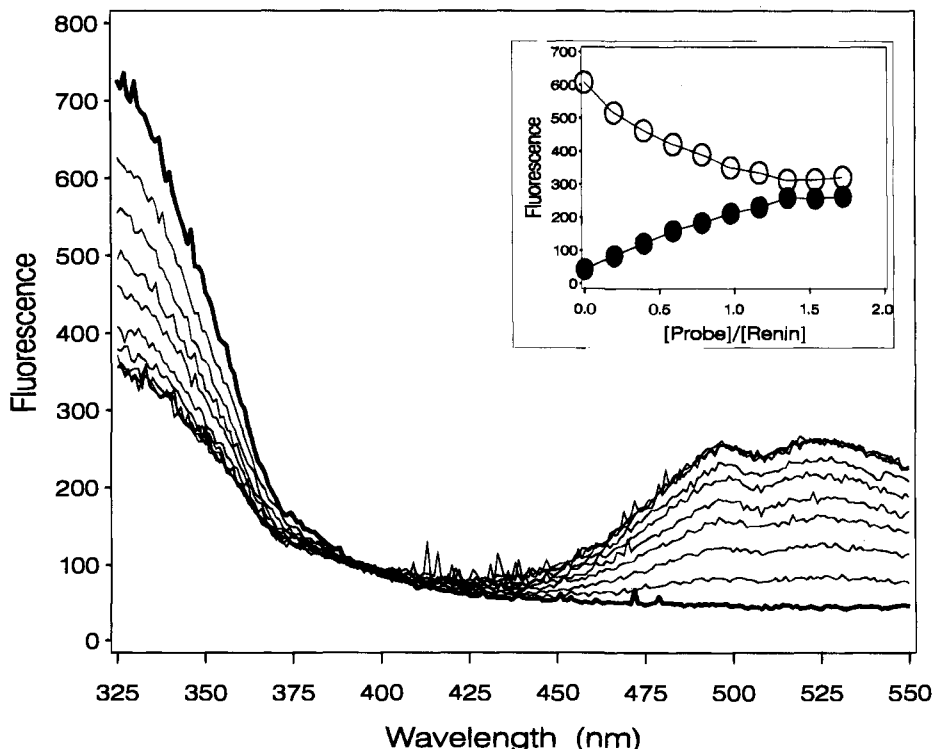
Figure 2. Emission spectra for renin and 1. Emission spectra are shown for the titration of 5.0×10^{-8} M renin (thick line) with successive aliquots of 1.0×10^{-8} M 1 (thin lines). The excitation wavelength was 284 nm with a band-pass of 1 nm; the emission band-pass was 16 nm. Inset: Fluorescence at 340 nm (open circles) and 520 nm (closed circles) is shown for each aliquot of added 1.
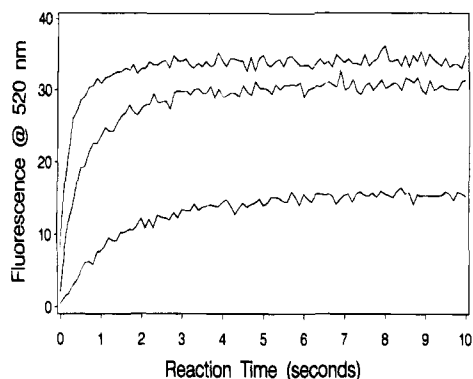
Figure 3. Association of 1 with renin. Fluorescence emission at 520 nm is shown for the association of renin (5.0×10^{-8} M) with various concentrations of 1 in a stopped-flow reactor: 5.0 $\times$ 10^{-7} M, top curve; 2.5×10^{-7} M, middle curve; and 5.0 $\times$ 10^{-8} M, bottom curve. Data was acquired for 10 s with an acquisition time of 100 ms. Each curve is the average of three separate experiments.

with a K_I of 12 nM. In the second step, EI is converted into a more tightly bound complex, EI*, with an overall K_I^* of 190 pM. These two steps will be observed separately *only* when (1) [I] is on the same order of magnitude as K_I and (2) the rapid collision step (usually diffusion-controlled at 10^7–10^8 M^{-1} s^{-1}) is slow enough to be detected by the techniques being employed; otherwise, the two steps will be perceived as one, defined by the rate-limiting step. Since the efficiency of the Trp → dansyl energy transfer is a sensitive function of distance ($1/r^6$ dependence[7]), a rapid collision complex should result in a maximum change in fluorescence within a few milliseconds (assuming that the distances between the Trp and dansyl fluorophores are approximately equal in the EI and EI* complexes). Thus, the following possibilities exist (1) the relative quantum yield for the loosely bound EI complex is much lower than for the EI* complex and not detected, (2) the K_I for the rapid collision complex is much higher for the system reported herein (compared with Kati's observation), or (3) a rapid collision, intermediate complex is not occurring. In any of these cases, the kinetics observed in Figure 3 are descriptive of the formation of the tightly bound (EI*) complex. Consequently, these data were analyzed with a simple one-step mechanism.

As discussed in the Theory section, it is desirable to obtain k_{on} and k_{off} for the probe, as they will be used for all subsequent determinations of k_{on} and k_{off} for the inhibitors of interest. Appendix 2 outlines the model to determine k_{1f} and k_{1r} from a pair of probe reactions, namely, a simple association and a 'trapping' dissociation, i.e., dissociation of the probe in the presence of a large excess of a potent, nonlabeled inhibitor. Such a pair of reactions is shown in Figure 4. These two curves were modeled simultaneously using the equations given in Appendix 2, and the resulting parameter estimates were used to simulate a pair of progress curves which are overlaid on the data. Although the k_{on} of 6.85 $\times$ 10^6 M^{-1} s^{-1} is below the diffusion limit of 10^7–10^8 M^{-1} s^{-1} for the association of a small molecule with a protein,[8] it is still greater than 10^6 M^{-1} s^{-1} given for slow binding ligands[9] and may reflect the kinetics of a relatively large inhibitor, i.e., a multiconformational peptidomimetic versus a small molecule. The k_{off} of 2.96 $\times$ 10^{-4} s^{-1} (first-order $t_{1/2}$ of 39 min) gives a calculated K_D of 43.2 pM. These values for k_{1f} and k_{1r} were held
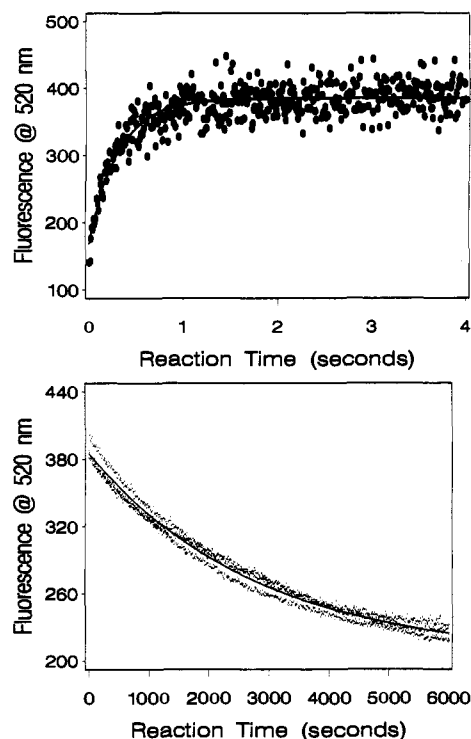

Figure 4. Association and dissociation of 1 with renin. Top panel: Association of 1 (5.0×10^{-7} M) with renin (5.0×10^{-8} M) in the stopped-flow reactor ($n = 3$). Bottom panel: Dissociation of 1 (5.0×10^{-7} M) from renin (5.0×10^{-8} M). The reactions ($n = 3$) were initiated by the addition of the trapping inhibitor 6 (3.1×10^{-5} M). Since the relative quantum yields are very different between stopped-flow cuvette reaction vessels, the association data were normalized to the amplitude ($F_{t=0} - F_{t=\infty}$) of the dissociation data (approximation by simple first-order decay). Both data sets were analyzed simultaneously, and nonlinear regression analysis converged to the following solution (solid lines): k_{on} = 6.85(0.18) $\times$ 10^6 M^{-1} s^{-1}, k_{off} = 2.96(0.11) $\times$ 10^{-4} s^{-1}, K_I(6) = 5.01(0.67) $\times$ 10^{-10}, where values in parentheses are the standard errors; see Appendix 2 for the kinetic model.

constant for all calculations involving 1 in paired ligand exchange reactions with the inhibitors of interest. Note that in the paired receptor–ligand exchange reactions, *vide infra*, the concentrations of inhibitor and probe are adjusted experimentally so that [EI]$_\infty$ $\approx$ [ED]$_\infty$ $\approx$ 0.5 [E]$_T$, insuring equal signal responses for both reactions. An expression for the limits of the assay can be derived for this experimental protocol using eqs 2 and 3 to give $K_I = ([I]_T/[D]_T)K_D$. For a peptide solubility limit of 5 $\times$ 10^{-5} M and degenerate ligand conditions ([I]$_T$ and [D]$_T$ $\geq$ 10[E]$_T$ = 5 $\times$ 10^{-7} M), the upper and lower limits for K_I would be 4300 and 0.43 pM, respectively, giving 4 orders of magnitude in sensitivity.

A typical example of a paired ligand exchange reaction involving 1 and 9 is shown in the top panel of Figure 5. In the top curve, renin was preincubated for about 5 min with 1 (association reactions are complete within seconds, *vide supra*) and 9 was added to initiate the exchange reaction; this reaction yields information principally concerning the k_{off} of 1 and the k_{on} of 9 (see eq 4). In the reverse reaction, renin was preincubated with 9 and 1 was added to initiate the exchange reaction; this complementary reaction yields information principally concerning the k_{off} of 9 and the k_{on} of 1 (see eq 5). Since the concentrations of the reactants are the same in each reaction, both curves should (and do) converge to the same fluorescence at equilibrium, i.e.,
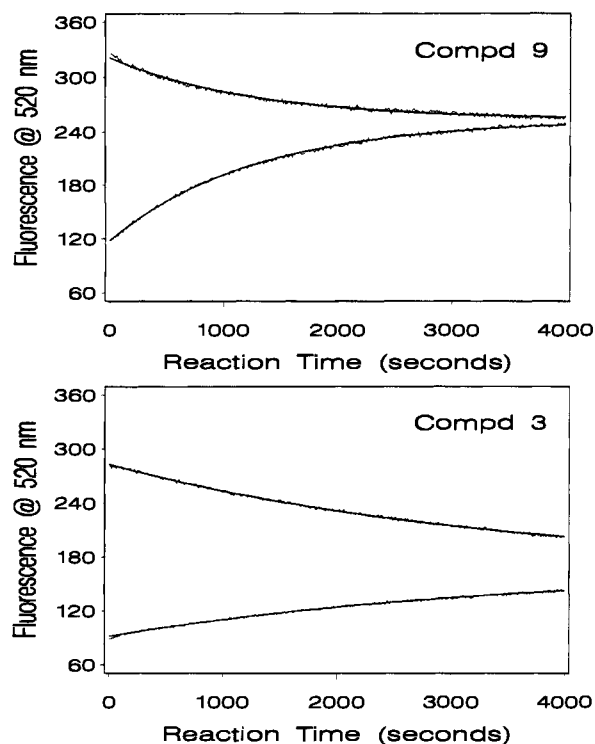
Figure 6. Renin competitive equilibrium curve between 1 and **3**. Reactions containing renin $(5.0 \times 10^{-8}$ M), 1 $(5.0 \times 10^{-7}$ M), and a series of concentrations of **3** were prepared and allowed to come to equilibrium overnight. The excitation wavelength was 284 nm with a band-pass of 1 nm; the emission wavelength was 520 nm with a band-pass of 16 nm. Nonlinear regression analysis, using the model given in Appendix 3 with $K_D = 43.2$ pM, converged (solid line) giving $K_I = 4.89(\pm0.43) \times 10^{-11}$ M, $Q_{free} = 2.34(\pm0.07) \times 10^8$ M^{-1}, and $Q_{bound} = 4.79(\pm0.08) \times 10^9$ M^{-1}, where values in parentheses are the standard errors.

Figure 5. Paired ligand exchange reactions with renin between 1 and sample inhibitors. Top panel: In the top curve, dissociation of 1 from renin was initiated by the addition of **9** (see eq 4); in the reverse reaction (bottom curve), dissociation of **9** from renin was initiated by 1 (see eq 5). $[1] = 5.0 \times 10^{-7}$ M, $[9] = 1.35 \times 10^{-5}$ M, and [renin] $= 5.0 \times 10^{-8}$ M for both reactions. Nonlinear regression analysis converged to the solution (solid lines) given in Table 1 for **9**. The excitation wavelength was 284 nm with a band-pass of 1 nm; the emission wavelength was 520 nm with a band-pass of 16 nm. Bottom panel: Same as the top panel except that the sample inhibitor was **3** ([**3**] $= 8.60 \times 10^{-7}$ M).

$F_{t=\infty}$. The data from both reactions were modeled simultaneously using the equations given in Appendix 1, and the resulting parameter estimates (see Table 1) were used to simulate a pair of progress curves which are overlaid on the data. In a similar example, a paired reaction was obtained for **3** (Figure 5, bottom panel). The major kinetic difference between these two sample inhibitors is that k_{off} is over 1 order of magnitude lower for **3**. Since their k_{on} values are comparable (see Table 1), the experimental differences are manifested primarily in the lower curve of each pair, as lower k_{off} values result in slower exchange rates to equilibrium. Also note that the concentration of **3** required to achieve $[EI]_{\infty} \approx [ED]_{\infty} \approx 0.5$ $[E]_T$ is over 1 order of magnitude lower than that required for **9**, as per eqs 2 and 3. As a point added in proof, the K_I for **3** was independently determined by equilibrium displacement reactions. The resulting displacement curve was analyzed with an equilibrium model (see Figure 6 and Appendix 3), giving a K_I of 48.9 pM which agrees with the value of 47.2 pM obtained by the kinetic method (Table 1).

Similar results were obtained for the other inhibitors in the series which are listed in Table 1 in order of increasing k_{off}. The K_I values varied over 2 orders of magnitude, while the individual k_{on} and k_{off} constants varied only over 1 order of magnitude. Interestingly, the rank ordering of potency by K_I does *not* match the ordering by k_{off}. Thus, if the half-life of the inactive ligand—receptor complex were crucial for pharmacologi-
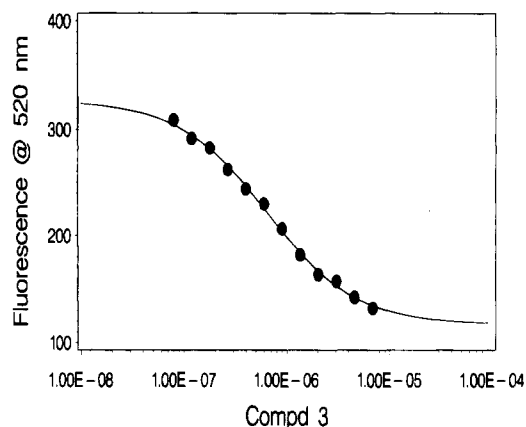
cal efficacy, some compounds which were ranked more potent by the equilibrium measurements K_I would actually be less effective than those exhibiting the higher K_I but lower k_{off} values.
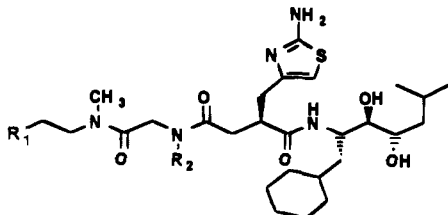
In conclusion, k_{on} and k_{off} rate constants were determined for a series of peptidomimetic, competitive inhibitors of renin using a novel binding assay in which a pair of receptor—ligand exchange reactions were carried out using a structurally related, fluorescent probe. Both reactions in the pair yielded progress curves which contain complementary information concerning the on and off rates of each ligands. The two curves were fitted simultaneously using a model derived from differential rate equations describing the ligand exchange process. In general, the paired ligand exchange method should be applicable to a wide range of receptor—ligand interactions in the exploration of rate phenomena.

Experimental Section

A. Synthesis and Characterization of the Probe (Compound 1). The synthesis of dansylated ligand 1, which employs $(2S,3R,4S)$-2-[$(tert$-butyloxycarbonyl)amino]-1-cyclohexyl-3,4-dihydroxy-6-methylheptane[10] as starting material, is shown in Scheme 1.

General Methods. NMR spectra were recorded on a Bruker AMX400 spectrometer and are referenced to TMS as internal standard. IR spectra were recorded on a Perkin-Elmer 781 spectrophotometer. CI and EI mass spectra were recorded on an MF 50 TATC instrument operating at 70 eV. Optical rotations were measured on a Perkin-Elmer 241 MC polarimeter at the sodium D line with a 1 dm path length, 1 mL cell. Flash chromatography was performed on Merck silica gel 60 (0.040—0.063 mm) using nitrogen pressure. Analytical thin-layer chromatography (TLC) was carried out on precoated (0.25 mm) Merck silica gel F-254 plates. All reactions were conducted under a positive nitrogen atmosphere in oven-dried glassware using standard syringe techniques. Diisopropylethylamine was distilled over calcium hydride. Solvents (obtained from BDH) were of Omnisolv quality and used without distillation.

2-[[N^{α}-Boc-N^{im}-(2,4-dinitrophenyl)-L-histidyl]amino]-1-cyclohexyl-3,4-dihydroxy-6-methylheptane (10). To a solution of $(2S,3R,4S)$-2-[$(tert$-butyloxycarbonyl)amino]-1-cy-

Table 1. Renin Inhibitor Rate Constants[a]

compd	R_1	R_2	$k_{on}(M^{-1}s^{-1})$	$k_{off}(M^{-1})$	$t_{1/2}(min)$[b]	$K_i(pM)$[c]
2			8.63(0.20)×10⁶	2.34(0.05)×10⁻⁴	49.4	27.1
3			5.93(0.17)×10⁶	2.80(0.08)×10⁻⁴	41.3	47.2
4			1.22(0.07)×10⁷	5.69(0.32)×10⁻⁴	20.3	46.6
5			2.00(0.08)×10⁶	1.30(0.05)×10⁻³	8.9	650
6			5.43(0.22)×10⁶	1.33(0.05)×10⁻³	8.7	245
7			6.68(0.17)×10⁶	1.35(0.03)×10⁻³	8.6	202
8			2.28(0.09)×10⁶	1.75(0.07)×10⁻³	6.6	768
9			2.07(0.12)×10⁶	4.81(0.27)×10⁻³	2.4	2320

[a] Determined by ligand exchange reactions at pH 7.4 with compound **1** as probe (see Appendix 1 for kinetic model). Values in parentheses are the asymptotic standard errors; Q_{bound} and Q_{free} (see eq 6 varied $< \pm 5\%$, and Δ (see eq 6a) varied $< \pm 5\%$ of the reaction amplitude, i.e., $F_{max} - F_{min}$. [b] Calculated from simple first-order decay ($t_{1/2} = \ln 2/k_{off}$). [c] Dissociation constant calculated from k_{off}/k_{on}.

Scheme 1
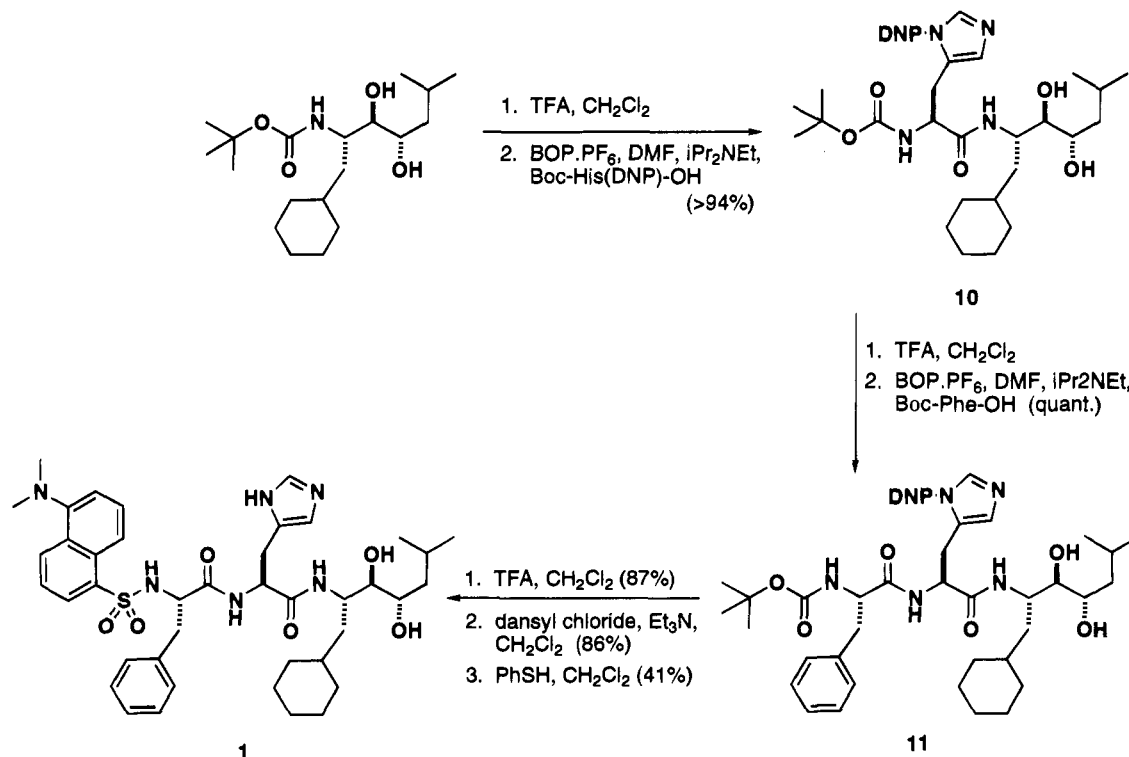
clohexyl-3,4-dihydroxy-5-methylhexane (500 mg, 1.45 mmol) in dichloromethane (7 mL) was added TFA (3 mL), and the resultant mixture was stirred for 1 h. Subsequently, the solvent was removed *in vacuo*, and the residue was dissolved in ethyl acetate. After washing with saturated aqueous sodium bicarbonate, the organic layer was dried (MgSO₄, anhydrous) and concentrated to give the corresponding amine

(434 mg), which was used in the coupling reaction without further purification. The residue of (2S,3R,4S)-2-amino-1-cyclohexyl-3,4-dihydroxy-6-methylheptane was dissolved in DMF (3 mL). To a solution of N^α-Boc-N^{im}-(2,4-dinitrophenyl)-L-histidine (697 mg, 1.45 mmol) in DMF was added (benzo-triazol-1-yloxy)tris(dimethylamino)phosphonium hexafluoro-phosphate (705 mg, 1.60 mmol), and the resultant mixture was

stirred for 5 min. Subsequently, the DMF solution containing (2S,3R,4S)-2-amino-1-cyclohexyl-3,4-dihydroxy-5-methylhexane was added followed by diisopropylethylamine (0.76 mL, 3.0 mmol). The resultant solution was stirred for 1 h and then concentrated *in vacuo*. After the residue was dissolved in ethyl acetate, the organic layer was washed successively with saturated aqueous sodium bicarbonate and brine and then dried (MgSO₄, anhydrous). After concentration, subjection of the crude material to flash column chromatography[11] on silica gel with chloroform/methanol as solvent system afforded **10** as a pale yellow amorphous solid (961 mg, >94%) with 89.1% homogeneity by reversed-phase HPLC (Vydac protein & peptide C$_{18}$ column; acetonitrile/water solvent system containing 0.06% TFA): ¹H NMR (400 MHz, CDCl₃) δ 8.85 (s, 1H), 8.58 (d, J = 8 Hz, 1H), 8.00 (s, 1H), 7.74 (d, J = 8 Hz, 1H), 7.62 (s, 1H), 6.98 (s, 1H), 6.57 (d, J = 10 Hz, 1H), 5.92 (br d, J = 6 Hz, 1H), 4.42–4.28 (m, 3H), 3.35–3.15 (m, 3H), 3.12–3.06 (m, 2H), 1.90–1.80 (m, 1H), 1.75–1.05 (m, 23H), 0.90 (d, J = 6 Hz, 3H), 0.94–0.79 (m, 1H), 0.81 (d, J = 6 Hz, 3H).

2-[[N^α-(N^α-Boc-L-phenylalaninyl)-N^{im}-(2,4-dinitrophenyl)-L-histidyl]amino]-1-cyclohexyl-3,4-dihydroxy-6-methylheptane (11). To a solution of **10** (961 mg, 1.36 mmol) in dichloromethane (30 mL) was added TFA (5 mL), and the resultant mixture was stirred for 1 h. After washing with saturated aqueous sodium bicarbonate, the organic layer was dried (MgSO₄, anhydrous) and concentrated to give the corresponding amine (690 mg, 93%), which was used in the coupling reaction without further purification. The residue of 2-[[N^{im}-(2,4-dinitrophenyl)-L-histidyl]amino]-1-cyclohexyl-3,4-dihydroxy-6-methylheptane was dissolved in DMF (3 mL) and added to a solution of Boc-L-phenylalanine (135 mg, 0.51 mmol) and benzotriazol-1-yloxy)tris(dimethylamino)phosphonium hexafluorophosphate (248 mg, 0.56 mmol) in DMF (7 mL). To the resultant solution was added diisopropylethylamine (0.76 mL, 4.35 mmol), and the reaction mixture was stirred for 1 h. Subsequently, the mixture was concentrated *in vacuo*, and the residue was dissolved in ethyl acetate. The organic layer was washed successively with saturated aqueous sodium bicarbonate and brine and then dried (MgSO₄, anhydrous). After concentration, subjection of the crude material to flash column chromatography on silica gel with chloroform/methanol as solvent system afforded **11** as an amorphous solid (454 mg, quantitative) with 74.9% homogeneity by reversed-phase HPLC (Vydac protein & peptide C$_{18}$ column; acetonitrile/water solvent system containing 0.06% TFA).

2-[[N^α-[N^α-[[5-(Dimethylamino)-1-naphthyl]sulfonyl]-L-phenylalaninyl]-N^{im}-(2,4-dinitrophenyl)-L-histidyl]amino]-1-cyclohexyl-3,4-dihydroxy-6-methylheptane (1). To a solution of **11** (454 mg, 0.53 mmol) in dichloromethane (20 mL) was added TFA (4 mL), and the resultant mixture was stirred for 1 h. After washing with saturated aqueous sodium bicarbonate, the organic layer was dried (MgSO₄, anhydrous) and concentrated to give the corresponding amine (318 mg, 87%), which was used in the coupling reaction without further purification. The residue of 2-[[N^α-(L-phenylalaninyl)-N^{im}-(2,4-dinitrophenyl)-L-histidyl]amino]-1-cyclohexyl-3,4-dihydroxy-6-methylheptane was dissolved in dichloromethane (10 mL), and to the resultant solution were added successively triethylamine (0.06 mL, 0.42 mmol) and 5-(dimethylamino)-1-naphthalenesulfonyl chloride (123 mg, 0.46 mmol). The resultant mixture was stirred for 24 h, washed successively with saturated aqueous sodium bicarbonate and brine, and then dried (MgSO₄, anhydrous). After concentration, subjection of the crude material to flash column chromatography on silica gel with chloroform/methanol as solvent system afforded the DNP-protected derivative of 1 as an amorphous solid (335 mg, 86%) with 80.4% homogeneity by reversed-phase HPLC (Vydac protein & peptide C$_{18}$ column; acetonitrile/water solvent system containing 0.06% TFA): ¹H NMR (400 MHz, CDCl₃) δ 9.89–9.83 (m, 2H), 8.55–8.50 (m, 3H), 8.03–8.00 (d, J = 7 Hz, 1H), 7.80 (d, J = 6 Hz, 1H), 7.78 (s, 1H), 7.72 (d, J = 7 Hz, 1H), 7.49 (dd, J = 6, 7 Hz, 1H), 7.10 (d, J = 6 Hz, 1H), 7.00 (s, 1H), 6.94 (d, J = 7 Hz, 1H), 6.76–6.65 (m, 4H), 6.60 (d, J = 6 Hz, 1H), 5.22 (br s, 1H), 4.71 (q, J = 4 Hz, 1H), 4.38–4.30 (m, 2H), 3.60 (dd, J = 4, 8 Hz, 1H), 3.40–3.34 (m, 2H), 3.25–3.10

(m, 3H), 2.90–2.85 (m, 2H), 2.28 (br s, 1H), 1.97–1.86 (m, 1H), 1.70–1.36 (m, 10H), 1.22–1.12 (m, 1H), 1.05–0.71 (m, 14H).

To a cold (0 °C), stirred solution of the DNP-protected derivative of 1 (335 mg, 0.34 mmol) in DMF (5 mL) was added a 10% solution of thiophenol in dichloromethane (1 mL), and the resultant mixture was stirred for 90 min. Subsequently, the mixture was concentrated *in vacuo*. Subjection of the residue to successive flash column chromatography on silica gel (chloroform/methanol) and preparative reversed-phase HPLC (Whatman Partisil 10 ODS-3 column; acetonitrile/water solvent system containing 0.06% TFA) afforded the desired compound 1 as a TFA salt (125 mg). This material was dissolved in ethyl acetate, and the organic layer was washed with saturated aqueous sodium bicarbonate and dried (MgSO₄, anhydrous). Concentration of the solution gave the desired 1 as a pale yellow solid (105 mg, 41%) with homogeneities of 99.5% (Vydac protein & peptide C$_{18}$ column; acetonitrile/water solvent system containing 0.06% TFA) and 100% (Pharmacia C$_{18}$-C$_2$ column; acetonitrile/aqueous phosphate buffer, pH 7.4) by reversed phase HPLC: ¹H NMR (400 MHz, CDCl₃) δ 8.47 (d, J = 8 Hz, 1H), 8.00–7.94 (m, 2H), 7.88–7.80 (m, 1H), 7.45–7.37 (m, 1H), 7.25–7.10 (m, 1H), 7.09–7.02 (m, 2H), 6.75–6.53 (m, 6H), 4.79 (br s, 1H), 4.30 (br s, 1H), 3.70 (br s, 1H), 3.40 (br s, 1H), 3.30–3.17 (m, 3H), 3.05–2.97 (m, 1H), 2.92–2.80 (m, 6H), 2.62 (t, J = 12 Hz, 1H), 1.90 (br s, 1H), 1.75–1.30 (m, 10H), 1.20–1.00 (m, 5H), 0.99–0.75 (m, 11H); ¹³C NMR (100 MHz, CDCl₃) δ 174.0, 173.0, 151.8, 135.0, 134.5, 132.5, 131.0, 129.8, 129.1, 128.6, 128.1, 126.9, 122.9, 118.0, 115.2, 78.0, 69.9, 59.4, 54.0, 47.5, 45.4, 42.3, 38.6, 37.8, 33.7, 33.5, 32.5, 27.5, 26.5, 26.1, 24.7, 24.0, 21.7; HRMS calcd for C$_{41}$H$_{57}$N$_6$O$_6$S (MH$^+$) 761.40603, found 761.40284; [α]^{25}_D −134° (c 0.7, CHCl₃). Anal. Calcd for C$_{41}$H$_{56}$N$_6$O$_6$S·2H₂O: C, 61.78; H, 7.59; N, 10.55. Found: C, 62.19; H, 7.15; N, 10.71.

B. Reversed-Phase HPLC Homogeneities of Compounds 2-9. Compounds **2−9** were synthesized as reported by ref 3 (in-depth synthetic routes and physical characterizations will be reported elsewhere) and analyzed for their homogeneity by reversed-phase HPLC using two solvent systems. System 1: solvent system consisting of acetonitrile/water containing 0.06% TFA; Vydac C$_{18}$ column; spectrophotometric detection at 220 nm. System 2: solvent system consisting of acetonitrile/phosphate buffer, pH 7.4; Vydac C$_{18}$ or Pharmacia C$_{18}$-C$_2$ column; spectrophotometric detection at 220 nm. All compounds were found to be greater than 96% homogeneity by both HPLC systems. Results are as follows (compound; % homogeneity by system 1; % homogeneity by system 2): (**2**; 98.6; 95.6), (**3**; 99.0; 98.9), (**4**; >99.9; 98.9), (**5**; 98.9; 99.1), (**6**; 98.6; 98.8), (**7**; >99.9; 99.6), (**8**; 99.0; 98.5), (**9**; 98.2; 97.0).

C. Expression and Purification of Recombinant Human Renin. The cloning, expression, and production of recombinant human prorenin and the purification of recombinant human renin will be described in detail elsewhere.[12] Briefly, the full length cDNA for the human preprorenin was obtained by reverse transcription/PCR of total RNA prepared from human kidney. Stable and highly productive clones of recombinant human prorenin were established by DNA-mediated gene transfer of the human preprorenin cDNA under a strong CMV IE promoter into DAMP cells, an adherent dog epithelial cell line. For the large-scale production of recombinant prorenin, cells were cultured into Nunc cell factories (6800 cm²) and kept at confluence. This system had the capacity to produce 3−5 mg of recombinant human prorenin/L of culture medium.

Renin was purified from the trypsin-activated culture media using an affinity chromatography column consisting of Sepharose-4B coupled with the renin inhibitor Boc-Phe-His-ACHPA-Ile-His-Gly-OH (K$_i$ = 3 nM). Following a wash in 50 mM Tris, 5 mM EDTA, 0.1 mM PMSF, 1 M NaCl, pH 7.4, the enzyme was eluted with a 100 mM glycine buffer, pH 11. For some enzyme preparations, a gel filtration chromatography step (Superdex-75) was added to eliminate high molecular weight aggregates and resulted in a homogeneous preparation. Pure enzyme was stored at −80 °C at a concentration of 200 μg/mL in 150 sodium acetate, 5 mM EDTA, pH 6.0.

D. Spectroscopic and Computational Methods. Con-

ventional Fluorescence Spectroscopy. Reactions were conducted at 37 °C in a fluorescence quartz cuvette (1 cm light path) containing a 2.00 mL reaction volume composed of 10 mM HEPES, 0.15% n-octyl β-D-glucopyranoside, and 1% DMSO at a pH of 7.4. Renin, at a concentration of 5.0×10^{-8} M, was titrated with successive 1.0×10^{-8} M aliquots of the fluorescent probe 1 (see Figure 1), for the acquisition of fluorescence emission spectra. Kinetic rate constants were determined by ligand exchange experiments using 1 at 5.0×10^{-7} M and renin at 5.0×10^{-8} M. The concentrations of competing ligand (as shown in the figure legends) were selected to displace approximately 50% of the bound 1 at equilibrium. Renin and either 1 or the competing ligand were preincubated for 5 min in the sample chamber with stirring at 37 °C. An SLM Aminco Bowman series 2 luminescence spectrometer was used for fluorescence detection. The excitation and emission wavelengths were set as described in the figure legends. Fluorescence was recorded as the ratio of emitted light to the reference photodiode.

Stopped-Flow Fluorescence Spectroscopy. Rate constants for the association of fluorescent probe and recombinant human renin were determined using an SLM Aminco Bowman series 2 luminescence spectrometer with an attached MilliFlow stopped-flow reactor equipped with two 2.50 mL reaction syringes and a 1.00 mL exit syringe. One reaction syringe contained renin at a concentration of 1.0×10^{-7} M in 10 mM HEPES, 0.15% n-octyl glucoside at a pH 7.4, while the other contained fluorescent probe at various concentrations in the same buffer. Reactions were initiated by injecting 50 μL from each reaction syringe using 50 psi of nitrogen through a final reaction volume of 32 μL at a temperature of 37 °C. The excitation wavelength was set at 284 nm (band-pass = 4 nm) and the emission wavelength of 520 nm (band-pass = 16 nm) at 1200 V. Fluorescence is given as the ratio of emitted light to the reference photodiode. The acquisition delay was determined by the N-bromosuccinamide-catalyzed oxidation of N-acetyltryptophanamide[13] to be about 1.2 ms.

Nonlinear Regression Analysis. All of the data were analyzed using the SAS statistical software system (version 6.08; SAS Institute Inc., Cary, NC) on an HP Apollo 735 workstation (Hewlett-Packard Co., Palo Alto, CA). Typically, two ASCII data files containing fluorescence measurements from a pair of ligand exchange reactions (eqs 4 and 5) were converted into a single SAS data set, with the respective subsets labeled as 'Association' or 'Dissociation' (referring to the disposition of the probe, see the Theory section). Data analyses were performed by applying ordinary nonlinear least-squares regression techniques to the selected model (see Appendices 1–3) using the Marquardt–Levenberg minimization method.

Appendix 1: Paired Ligand Exchange Model

The following solution was derived for degenerate conditions on the probe where [ligand]$_{free}$ ≈ [ligand]$_{Total}$, i.e., $[D] \approx [D]_T$. The differential rate equations for the enzyme species in the overall ligand exchange reaction (eq 1) are

$$\frac{d[ED]}{dt} = (k_{1f}[E][D]) - (k_{1r}[ED]) \qquad (7)$$

$$\frac{d[E]}{dt} = (k_{1r}[ED]) - (k_{1f}[E][D]) + (k_{2r}[EI]) - (k_{2f}[E][I]) \qquad (8)$$

$$\frac{d[EI]}{dt} = (k_{2f}[E][I]) - (k_{2r}[EI]) \qquad (9)$$

Solution for [E]$_t$. An expression for d[E] suitable for integration can be obtained by first substituting mass balance expression for [EI] $(= [E]_T - [E] - [ED])$ into eq 8, solving for [ED], and substituting into eq 7 to give

$$\frac{d[ED]}{dt} = k_{1f}[E][D]_T - k_{1r} \times$$

$$\left\{ \frac{\frac{d[E]}{dt} + [((k_{1f}[D]_T) + k_{2r} + (k_{2f}[I]_T))[E]] - (k_{2r}[E]_T)}{k_{1r} - k_{2r}} \right\} \qquad (10)$$

Again with eq 8, substitution of mass balance for [EI], differentiation with respect to t, and substitution of d[ED]/dt from eq 10 results in the following expression:

$$a \frac{d^2[E]}{dt^2} + b \frac{d[E]}{dt} + c[E] = d \qquad (11)$$

where

$$a = 1$$

$$b = k_{1r} + (k_{1f}[D]_T) + k_{2r} + (k_{2f}[I]_T)$$

$$c = k_{1r}((k_{1f}[D]_T) + k_{2r} + (k_{2f}[I]_T)) - (k_{1r} - k_{2r})k_{1f}[D]_T$$

$$d = k_{1r}k_{2r}[E]_T$$

This is a nonhomogeneous differential equation of second order and first degree with a single dependent variable. The following solution can be obtained by applying the 'variation of parameters' method:[14]

$$[E]_t = \frac{k_{1r}k_{2r}[E]_T}{\varrho_1\varrho_2} + \lambda_1 e^{-\varrho_1 t} + \lambda_2 e^{-\varrho_2 t} \qquad (12)$$

where

$$\varrho_{1,2} = \frac{b \pm \sqrt{b^2 - 4ac}}{2a}$$

λ_1 and λ_2 are defined from boundary conditions, and ϱ_1 and ϱ_2 are the positive and negative roots, respectively. For $t = \infty$,

$$[E]_\infty = \frac{k_{1r}k_{2r}[E]_T}{\varrho_1\varrho_2} \qquad (12a)$$

For $t = 0$,

$$\lambda_2 = [E]_0 - [E]_\infty - \lambda_1 \qquad (12b)$$

Solutions for λ_1 and λ_2 are obtained by first taking the derivative of eq 12 with respect to time and setting $t = 0$.

$$\left(\frac{d[E]}{dt}\right)_{t=0} = -\varrho_1\lambda_1 - \varrho_2\lambda_2 \quad (13)$$

From eq 8 at $t = 0$,

$$\left(\frac{d[E]}{dt}\right)_{t=0} = (k_{1r}[ED]_0) - (k_{1f}[E]_0[D]_0) + \\ (k_{2r}[EI]_0) - (k_{2f}[E]_0[I]_0) \quad (14)$$

Equating eq 13 with eq 14 and substituting eq 12b for λ_2 lead to

$$\lambda_1 = [[E]_0((k_{1f}[D]_T) + (k_{2f}[I]_T) - \varrho_2) + (\varrho_2[E]_\infty) - \\ (k_{1r}[ED]_0) - (k_{2r}[EI]_0)]/(\varrho_1 - \varrho_2) \quad (15)$$

For the paired ligand exchange reaction involving probe dissociation (eq 4), $[EI]_0 = 0$ and $[ED]_0 = $ quadratic solution. For the complementary probe association reaction (eq 5), $[ED]_0 = 0$ and $[EI]_0 = $ quadratic solution. Substituting eqs 12a,b into eq 12, the fully evaluated expression for $[E]$ at time t may now be rewritten as follows:

$$[E]_t = [E]_\infty + \lambda_1 e^{-\varrho_1 t} + ([E]_0 - [E]_\infty - \lambda_1)e^{-\varrho_2 t} \quad (16)$$

[Note: A simpler expression for $[E]_t$ exists if the assumption can be made that the enzyme will be saturated with ligand at all times. Under these conditions, the alternative enzyme–inhibitor complex will always be formed at the expense of the preformed one. An immediate result of this experimental protocol is that $d[E]/dt$ is always a very small number. Thus, $[E]_t$ can be approximated by setting $d[E]/dt$ (eq 8) equal to zero. This solution is known as the Bodenstein approximation,[15] more commonly referred to as the steady or stationary state approximation. The model breaks down, however, for ligands whose K_d and experimental solubility do not allow saturation of the receptor.]

Solution for $[ED]_t$. An expression for $d[ED]$ suitable for integration may be obtained by substituting eq 16 into eq 7 and rearranging:

$$\frac{d[ED]}{dt} + k_{1r}[ED] = k_{1f}[D]_T([E]_\infty + \lambda_1 e^{-\varrho_1 t} + \\ ([E]_0 - [E]_\infty - \lambda_1)e^{-\varrho_2 t}) \quad (17)$$

Integration of this first-order linear differential equation[14] leads to the following solution for $[ED]$ at time t.

$$[ED]_t = k_{1f}[D]_T\left\{\frac{[E]_\infty}{k_{1r}} + \frac{\lambda_1}{k_{1r} - \varrho_1}e^{-\varrho_1 t} + \\ \frac{([E]_0 - [E]_\infty - \lambda_1)}{k_{1r} - \varrho_2}e^{-\varrho_2 t}\right\} + C_i e^{-k_{1r}t} \quad (18)$$

where C_i is the constant of integration. For $t = 0$,

$$C_i = [ED]_0 - k_{1f}[D]_T\left\{\frac{[E]_\infty}{k_{1r}} + \frac{\lambda_1}{k_{1r} - \varrho_1} + \\ \frac{([E]_0 - [E]_\infty - \lambda_1)}{k_{1r} - \varrho_2}\right\} \quad (18a)$$

For $t = \infty$,

$$[ED]_\infty = \frac{k_{1f}[D]_T[E]_\infty}{k_{1r}} \quad (18b)$$

Regression. To obtain the expressions for modeling the fluorescence data, $[ED]_t$ from eq 18, as defined by association or dissociation of the probe, is substituted into eqs 6 and 6a, respectively. In the fitting procedure, k_{1f}, k_{1r}, $[D]_{Total}$, and $[E]_{Total}$ are held constant while k_{2f}, k_{2r}, Q_{free}, Q_{bound}, and Δ are determined by regression.

Appendix 2: Model for Determining the Probe Rate Constants

The following solutions were derived for nondegenerate ligand conditions where [ligand]$_{free}$ may not be assumed to compare with [ligand]$_{Total}$. Consequently, explicit mass balance relationships were used.

k_{on} **for Probe.** Consider the following association reaction of the probe with enzyme.

$$E + D \underset{k_{1r}}{\overset{k_{1f}}{\rightleftharpoons}} ED \quad (19)$$

The equilibrium expression and the differential rate equations for the reaction between a fluorophoric inhibitor (D) and enzyme (E) are given by eqs 2 and 7, respectively. Substitution of k_{1r} from eq 2 and mass balance expression for $[E]$ into eq 7 and separation of the variables lead to the following integral:

$$\int_{[ED]_0}^{[ED]_t}\frac{d[ED]}{c[ED]^2 + b[ED] + a} = -k_{1f}\int_{t=0}^{t=t}dt \quad (20)$$

where

$$a = -[E]_T[D]_T$$

$$b = [E]_T + [D]_T + \frac{k_{1r}}{k_{1f}} \quad (20a)$$

$$c = -1$$

Integration[16] results in the following solution for $[ED]$ at time t:

$$\ln\frac{(2c[ED]_t) + b - \sqrt{-q}}{(2c[ED]_t) + b + \sqrt{-q}} = -(\beta t) + C_i \quad (21)$$

where

$$q = (4ac) - b^2$$

$$\beta = k_{1f}\sqrt{-q}$$

A solution for the constant of integration may be obtained by setting $t = 0$,

$$C_i = \ln\frac{(2c[ED]_0) + b - \sqrt{-q}}{(2c[ED]_0) + b + \sqrt{-q}} \quad (21a)$$

Solving eq 21 for $[ED]$ at time t,

$$[ED]_t = \frac{-b + \sqrt{-q} + ((b + \sqrt{-q})\gamma_i e^{-\beta t})}{2c(1 - \gamma_i e^{-\beta t})} \quad (22)$$

where γ_i is the antilog of C_i.

For $t = 0$,

$$[ED]_0 = \frac{-b + \sqrt{-q} + ((b + \sqrt{-q})\gamma_i)}{2c(1 - \gamma_i)} \quad (22a)$$

For $t = \infty$,

$$[ED]_\infty = \frac{-b + \sqrt{-q}}{2c} \quad (22b)$$

Rearrangement of eq 22 and substitution of eqs 22a,b lead to

$$[ED]_t = \frac{[ED]_\infty + (([ED]_0(1 - \gamma_i)) - [ED]_\infty)e^{-\beta t}}{1 - \gamma_i e^{-\beta t}} \quad (23)$$

For the forward (association) reaction, $[ED]_0 = 0$ by definition.

k_{off} for Probe. Following the above scheme, the reverse reaction would be carried out by first preincubating E and D at high concentrations and then initiating dissociation by diluting to lower concentration. Preliminary calculations based on eq 23, however, indicated that the amount of dissociation (thus, signal) would be so small as to make this experimental design impractical. However, consider the following reaction in which a nonfluorophoric inhibitor is used to drive the equilibrium for the probe dissociation far to the right:

$$ED + \text{excess I} \overset{k_{1f}}{\underset{k_{1r}}{\rightleftharpoons}} EI + D \quad (24)$$
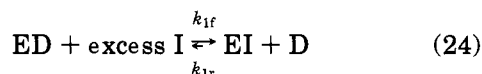
Although this reaction is similar to eq 4, it differs in that $[EI]_\infty \gg [ED]_\infty$. Thus, as D dissociates, free E will be instantaneously 'trapped' by I, blocking any reassociation of probe, so that a measurable dissociation reaction can be analyzed. The solution (assuming instantaneous equilibrium with I) derived for this trapping exchange reaction is similar to the expression obtained above for the simple association of E + D. From eqs 3 and 7,

$$\frac{d[ED]}{dt} = \left(k_{1f} \frac{[EI]K_I}{[I]_T}[D] \right) - k_{1r}[ED] \quad (25)$$

Assuming that E is saturated with either D or I under the experimental conditions employed, EI will be formed at the expense of ED so that $[EI]_t = [ED]_0 - [ED]_t$. Substituting for $[EI]_t$ and mass balance relationships for [D] and separation of the variables lead to the integral given by eq 20 where

$$a = -\frac{K_I[ED]_0[D]_T}{[I]_T}$$

$$b = \frac{K_I[D]_T}{[I]_T} + \frac{K_I[ED]_0}{[I]_T} + \frac{k_{1r}}{k_{1f}} \quad (26)$$

$$c = -\frac{K_I}{[I]_T}$$

The final solution for $[ED]_t$ is completely analogous to the derivation and expression given by eq 23.

Regression. To obtain the expressions for modeling the fluorescence data, $[ED]_t$ from eq 23, as defined by association (eq 20a) or dissociation (eq 26) of the probe, is substituted into eqs 6 and 6a, respectively. In the fitting procedure, $[D]_{Total}$ and $[E]_{Total}$ are held constant while k_{1f}, k_{1r}, K_I, Q_{free}, Q_{bound}, and Δ are determined by regression.

Appendix 3: Model for Determining the Equilibrium Constant

This model describes the equilibrium given in eq 1 and assumes degenerate conditions for D and nondegenerate for I. Substituting eq 3 for [E] into eq 2 and the mass balance relationship for [I] leads to

$$[EI] = \frac{K_D[I]_T[ED]}{(K_D[ED]) + (K_I[D]_T)} \quad (27)$$

Substituting into the mass balance relationship for $[E]_T$ gives

$$[E]_T = \frac{K_D[ED]}{[D]_T} + [ED] + \frac{K_D[I]_T[ED]}{(K_D[ED]) + (K_I[D]_T)} \quad (28)$$

Solving for [ED] leads to a quadratic equation

$$a[ED]^2 + b[ED] + c = 0 \quad (29)$$

where

$$a = \left(\frac{K_D}{[D]_T} + 1 \right) K_D$$

$$b = \left\{ \left(\frac{K_D}{[D]_T} + 1 \right) K_I[D]_T \right\} + (K_D[I]_T) - (K_D[E]_T) \quad (29a)$$

$$c = -(K_I[D]_T[E]_T)$$

To obtain the expression for modeling the fluorescence data, the positive root of the quadratic solution for [ED] is substituted into eq 6. In the fitting procedure, $[I]_T$ and $F_{t=\infty}$ are the independent and dependent parameters, respectively, $[D]_{Total}$, $[E]_{Total}$, and K_D are held constant, and K_I, Q_{free}, and Q_{bound} are determined by nonlinear regression. Figure 6 shows a renin competitive equilibrium curve between **1** and **3**. The $K_I(3)$ of $4.89(\pm0.43) \times 10^{-11}$ M compares well with the value of 47.2 pM obtained by the kinetic method (Table 1).

References

(1) Epps, D. E.; Poorman, R. A.; Mandel, F.; Schostarez, H. J. Determination of Dissociation Constants of High Affinity (pM) Human Renin Inhibitors: Application to Analogues of Ditekiren (U-71,038). *J. Med. Chem.* **1991**, *34*, 2107–2112. Epps, D. E.; Schostarez, H.; Argoudelis, C. V.; Poorman, R.; Hinzmann, J.; Sawyer, T. K.; Mandel, F. An Experimental Method for the Determination of Enzyme-Competitive Inhibitor Dissociation Constants from Displacement Curves: Application to Human Renin using Fluorescence Energy Transfer to a Synthetic Dansylated Inhibitor Peptide. *Anal. Biochem.* **1989**, *181*, 172–181. Epps, D. E.; Poorman, R.; Hui, J.; Carlson, W.; Heinrikson, R. Inaccessibility of Tryptophan Residues of Recombinant Human Renin to Quenching Agents. *J. Biol. Chem.* **1987**, *262*, 10570–10573.

(2) Kaplan, A. P.; Bartlett, P. A. Synthesis and Evaluation of an Inhibitor of Carboxypeptidase A with a Ki Value in the Femptomolar Range. *Biochemistry* **1991**, *30*, 8165–8170.

(3) Lavallee, P.; Simoneau, B. Renin Inhibiting N-(2-Amino-2-oxoethyl)butanediamide Derivatives. European Patent 589445, 1994. Anderson, P. C.; Bruno, S.; Halmos, T.; Jung, G. L.; Poupart, M.; Simoneau, B. N-(Hydroxyethyl)butanediamide Derivatives as Renin Inhibitors. European Patent 589446, 1994.

(4) Abdel-Meguid, S. S. Inhibitors of Aspartyl Proteinases. *Med. Res. Rev.* **1993**, *13*, 731−778. Hutchins, C.; Greer, J. Comparative Modeling of Proteins in the Design of Novel Renin Inhibitors. *Crit. Rev. Biochem. Mol. Biol.* **1991**, *26*, 77−127. Kleinert, H. D.; Baker, W. R.; Stein, H. H. Renin Inhibitors. *Adv. Pharmacol.* **1991**, *22*, 207−250. Greenlee, W. J. Renin Inhibitors. *Med. Res. Rev.* **1990**, *10*, 173−236.

(5) Pargellis, C. A.; Morelock, M. M.; Graham, E. T.; Kinkade, P.; Pav, S.; Lubbe, K.; Lamarre, D.; Anderson, P. C. Determination of Kinetic Rate Constants for the Binding of Inhibitors to HIV-1 Protease and for the Association and Dissociation of Active Homodimer. *Biochemistry* **1994**, *33*, 12527−12534.

(6) Kati, W. M.; Pals, D. T.; Thaisrivongs, S. Kinetics of the Inhibition of Human Renin by an Inhibitor Containing a Hydroxyethylene Dipeptide Isostere. *Biochemistry* **1987**, *26*, 7621−7626.

(7) Lakowicz, J. R. *Principles of Fluorescence Spectroscopy*; Plenum Press: New York, 1983; pp 305−339.

(8) Hanson, J. E.; Kaplan, A. P.; Bartlett, P. A. Phosphonate Analogues of Carboxypeptidase A Substrates are Potent Transition-State Analogue Inhibitors. *Biochemistry* **1989**, *28*, 6294−6305.

(9) Bartlett, P. A.; Hanson, J. E.; Giannousis, P. P. Potent Inhibition of Pepsin and Penicillopepsin by Phosphorus-Containing Peptide Analogues. *J. Org. Chem.* **1990**, *55*, 6268−6274.

(10) Luly, J. R.; BaMaung, N.; Soderquist, J.; Fung, A. K.; Stein, H.; Kleinert, H. D.; Marcotte, P. A.; Egan, D. A.; Bopp, B.; Merits, I.; Bolis, G.; Greer, J.; Perun, T. J.; Plattner, J. J. Renin Inhibitors: Dipeptide Analogues of Angiotensinogen Utilizing a Dihydroxyethylene Transition-state Mimic at the Scissile bond to Impart Greater Inhibitory Potency. *J. Med. Chem.* **1988**, *31*, 2264−2276.

(11) Still, W. C.; Kahn, M.; Mitra, A. Rapid Chromatographic Technique for Preparative Separations with Moderate Resolution. *J. Org. Chem.* **1978**, *43*, 2923−2925.

(12) Pilote, L.; McKercher, G.; Thibeault, D.; Lamarre, D. Enzymatic Characterization of Purified Recombinant Human Renin. *Biochem. Cell Biol.* **1995**, in press.

(13) Peterman, B. F. Measurement of the Dead Time of a Fluorescence Stopped-Flow Instrument. *Anal. Biochem.* **1979**, *93*, 442−444.

(14) Thomas, G. B. *Calculus and Analytical Geometry*, 4th ed.; Addison-Wesley: Reading, MA, 1969; pp 694−695, 701.

(15) Schmid, R.; Sapunov, V. N. *Monographs in Modern Chemistry: Non-formal Kinetics*; Verlag Chemie: Deerfield Beach, FL, 1982; pp 2−37. Hammett, L. P. *Physical Organic Chemistry: Reaction Rates, Equilibria, and Mechanisms*, 2nd ed.; McGraw-Hill: New York, NY, 1970; pp 53−100. Bodenstein, M. *Z. Physik. Chem.* **1913**, *85*, 329.

(16) Selby, S. M. *CRC Handbook Series: Standard Mathematical Tables*, 19th ed.; The Chemical Rubber Co., Cleveland, OH, 1971; pp 395, 403−404.